TD-05-051
October 14, 2005

MAGNETIZATION OF HIGH-J_C NB_3SN STRANDS

D. Turrioni[1], E. Barzi[1], M. Bossert[1], V.V. Kashikhin[1], A.V. Zlobin[1]

[1] Fermi National Accelerator Laboratory
Batavia, Illinois 60510, USA

ABSTRACT

The magnetization of Nb_3Sn strands used in Fermilab's high field magnets was measured at low (0-3-0 T) and high fields (10-13-10 T). The strands were produced using the Restack Rod Process (RRP) and Powder-in-Tube (PIT) technologies. Both round and deformed strands were studied. Measurements at high field were done in order to determine the effective filament size of strands. These results were compared with the filament sizes measured on cross-sections of round and deformed strands. Measurements at low fields were performed to study magnetic instabilities (flux jumps) in different Nb_3Sn strands. Effects of strand deformation as well as test temperature on strand magnetization were studied. This paper describes the Nb_3Sn strand samples, the equipment and measurement procedures, and the results of the magnetization measurements at low and high fields.

KEYWORDS: Nb_3Sn, Rutherford cable, magnetization, magnetic stability.
PACS: 74.70.Ad.

INTRODUCTION

Magnetic instabilities and field quality in Nb_3Sn accelerator magnets depend on the effective filament diameter, d_{eff}, of a superconducting strand [1,2]. One of the objectives of this work was to correlate the d_{eff} of Nb_3Sn strands of various technologies with their geometrical filament size. This was done first for round strands. The d_{eff} was calculated from 13-10-13 T magnetization loops by measuring $\mu_0\Delta M(12T)$ per total strand volume and $I_c(12T)$ [3]. Distributions of the geometric filament sizes were obtained using a high-resolution optical microscope. Since in high field accelerator magnet applications strands are subject to cabling, another important objective was to check for any changes in filament size distributions due to strand deformations during the cabling process. A number of rectangular and keystoned Rutherford cables made of different Nb_3Sn strands were used to measure the filament size

distributions of the deformed strands in the cables cross sections. Whereas substantial changes in both the average filament sizes and their standard deviations were found, this was not apparent from magnetization measurements. To better understand the role of d_{eff} in instabilities [4] and to simulate cabling deformations, the same strands used in the cables were rolled down to various sizes aiming at deformation values larger than 50%, and the filament size distributions were measured. In this case the average filament sizes and distribution widths changed substantially, and the effect could also be measured through magnetization. Finally, some RRP strands were tested also below and above 4.2 K to check instability behavior at different temperatures.

THE EXPERIMENT

Strands and Cables Description

Four different multifilamentary Restacked Rod Process (RRP) strands by Oxford Superconducting Technology (OST), and two Powder-in-Tube (PIT) Nb_3Sn strands by ShapeMetal Innovation (SMI), were studied. The strands parameters are summarized in Table I. Fig. 1 shows the three RRP strands designs. The RRP strands 7054-60 were used to fabricate 38 and 39-strand Rutherford cables at LBNL, whereas PIT strands were used to fabricate 28-strand cables at FNAL. The cables description is in Table 2 and a cross section is shown in Fig. 2. To expand the range of d_{eff} in strands and to compare strand and cable measurements, some strands were rolled down (before reaction) as shown in Fig. 2 (right) to various sizes.

Sample Preparation and Measurement Procedure

Samples for the magnetization measurements are wound on stainless steel tubes of about 1 cm in diameter and 3 inches long, as shown in Fig. 3 (left). The samples are heat treated in an Argon atmosphere according to optimal schedules for each technology. After reaction the sample is slid out of the tube and slipped on a G10 holder. Fig. 3 (center) shows a sample ready for test.

Magnetization measurements are performed using a balanced coil magnetometer. Typical cycles are between 0 and 3 T, and between 10 and 13 T, with a magnetic field ramp rate of 17 mT/s. The uncertainty on magnetization is ±1% at 1 T, less than ±4% at 12 T, and within ±6% on the effective filament diameter, d_{eff} [5]. Voltage-current (V-I) characteristics were measured at 4.2 K, in a transverse magnetic field. The voltage is measured along the sample by means of voltage taps placed 50 and 75 cm apart. The critical current I_c is determined using the 10^{-14} Ω·m resistivity criterion. The I_c measurement uncertainty is typically within ±1 % at 4.2 K and 12 T.

The geometric filament sizes were obtained using a high-resolution optical microscope equipped with an imaging software that allows measuring lengths with pixel resolution, i.e. 0.72 μm. For each strand, the short and long diameters were measured for all filaments on a number of cross sections as shown in Fig. 3 (right) with a precision of ±1 μm. The estimated accuracy was $\pm^{0}_{2.5\%}$. Due to the cables lay angle of ~14.5 degree, filament sizes measured on cable cross sections were overestimated by ~3% when parallel to the cable axis. Another systematic effect is to be considered in the case of the RRP study, since filament size distributions were obtained on reacted strands and unreacted cables. After reaction, the short

and long size of filaments in the RRP strand shrunk by 4.7 and 6 % respectively.

RESULTS AND DISCUSSION

Effective Filament Diameters and Geometric Filament Sizes

The effective filament diameters were obtained from 13-10-13 T loops by measuring $\mu_0\Delta M(12T)$ per total strand volume and the $I_c(12\ T)$, and considering the filaments round. Results for the six round strands are shown in Table 3, which also includes the two values obtained for the geometric filament sizes. The first value is the average of the short diameters, the second value is the average of the long diameters. One can see that in the case of the RRP strands, the d_{eff} is always 10 to 13% larger than the long and 33 to 39% larger than the short average geometric size, whereas in the case of the PIT strands the d_{eff} is smaller or the same as the smallest geometric size, which makes sense since the Nb tube does not react through. An explanation for d_{eff}'s larger than the geometric size of the filaments can be found in [6]. By extrapolating the data shown in Fig. 4, a 217-filament strand design would provide a d_{eff} of 24 μm for a 0.7 mm strand and of ~34 μm for a 1 mm strand.

For each deformed strand in the cables cross sections, the short and long diameters were also measured for all filaments. Both the average and the standard deviation of the long diameters distributions were found to be larger in cabled strands with respect to round, as can be seen in Figs. 5 and 6. In the case of the RRP unreacted cables this increase was 2 to 6% after a 6% adjustment for filament shrinkage during reaction, and no observable difference was found between keystoned and rectangular cables. In the case of the reacted PIT cables the increase was 9% for the rectangular geometry and 16% for the keystoned geometry. However, for both strand technologies the maximum filament sizes (112 μm for the RRP after a 6% adjustment, and 105 μm for the PIT) were found in rectangular cable cross sections.

To better understand the role of d_{eff} in instabilities and to simulate cabling deformations, the strands used in the cables were rolled down to various sizes aiming at deformation values larger than 50%. The average filament deformation of the short and long diameters are shown in Fig. 7 as a function of relative strand deformation for both RRP and PIT strands. The long diameter distributions of the rolled strands are shown in Figs. 5 and 6. It appears that a 20% deformation best represents the cabling behavior of the PIT strand, whereas in the case of the RRP strand this is achieved by a 10% deformation.

Effect of Cabling on Magnetization

Magnetization was measured for a round RRP strand and one extracted from a 39-strand keystoned cable at low and high fields (Fig. 8). The magnetization amplitude is nearly the same, but flux jumps are seen up to higher fields in the extracted strand. Since the d_{eff} changes only locally in the extracted strand, the contribution to magnetization is negligible, whereas instabilities are generated locally and presumably propagate along the strand.

Effect of Rolling on Magnetization

Magnetization was measured for a 1 mm PIT round strand and for the same strand rolled down to various sizes. The rolled strands were wound on the test holder with the long edge parallel to the field, hence with the shortest size of the filaments perpendicular to the field.

Low field results are shown in Fig. 9. It is interesting to observe that whereas the amplitude of flux jumps decreases considerably with decreasing rolled size, they appear in approximately the same magnetic field range. This phenomenon might be explained by the maximum short diameter being about the same for all rolled strands, whereas the average short diameter decreasing considerably (see Fig. 7), thereby reducing the volume of the unstable filaments.

In Fig. 10 (left) both $\Delta M(12\ T)$ and d_{eff} are plotted as a function of relative strand deformation. In Fig. 10 (right) the I_c (12 T) and n-value (15 T) are plotted, also as a function of relative strand deformation. It is interesting to notice that whereas $\Delta M(12\ T)$ also follows a parabolic law, albeit steeper than that of the geometrical filament size in Fig. 7, the d_{eff} appears to be more or less constant down to 50% deformation, where the I_c is very degraded, but magnetization still large. This might be due to cracks in the filaments.

Effect of Temperature

Fig. 11 shows low and high field results for a 0.8 mm RRP strand at 2.2 K, 4.2 K and 10 K. Whereas no flux jumps are seen at 10 K, it is apparent that at 2.2 K the field range of magnetic instabilities is larger than at 4.2 K. The character of instabilities changes from 4.2 K to 2.2 K. Magnetization amplitude at 2.2 K should be larger than at 4.2 K, but this is not the case in the curve in Fig. 11, as if whereas at 4.2 K flux jumps are local and recover fully, at 2.2 K there is a permanent degradation. More magnetization curves of round RRP strands at 4.2 K and 2 K are shown in Fig. 12 (left), and round and rolled RRP strands at 4.2 K and 10.5 K (right). The same effect of non-recovery is apparent from Fig. 12 (left) at 2 K.

When measuring d_{eff} from the magnetization curves at various temperatures, it was found that whereas there is a good consistency between the d_{eff} obtained at 4.2 K and that obtained at colder temperatures, at ~10 K this is not the case. For the strand in Fig. 11, the d_{eff} was overevaluated by ~30% when calculated from $\Delta M(2\ T)$, and under evaluated by at least a factor of 4 when calculated from $\Delta M(12\ T)$.

SUMMARY

The d_{eff} of round Nb_3Sn strands of various technologies was compared with their geometrical filament size. It was found that in the case of the RRP strands, the d_{eff} is always 10 to 13% larger than the longest geometric size, whereas in the case of the PIT strands the d_{eff} is smaller or on the same order than the smallest geometric size. Filament sizes distributions of the deformed strands in the cables cross sections were also analyzed to check for any changes. Both the average and the standard deviation of the long diameters distributions were found to increase in cabled strands with respect to round. In the case of the RRP cables no observable difference was found between keystoned and rectangular cables. In the case of the PIT cables the increase was larger for the keystoned geometry. No changes were apparent from magnetization measurements. In the case of rolled strands the average filament sizes and distribution widths changed substantially, and the effect could also be measured through magnetization. It was found that a 20% deformation best represent the cabling behavior of the PIT strand, whereas in the case of the RRP strand this is achieved by a 10% deformation. Finally larger instabilities were found below 4.2 K for strands of d_{eff} as low as 72 μm.

ACKNOWLEDGMENTS

This work was supported by the U.S. Department of Energy. In addition, the authors would like to thank Dan Dietderich for the numerous cables that were fabricated at LBNL and that are part of this study.

REFERENCES

1. V.V. Kashikhin, A.V. Zlobin, "Magnetic Instabilities in Nb_3Sn Strands and Cables", IEEE Transactions on Applied Superconductivity, Volume 15, Issue 2, June 2005 Page(s):1621 – 1624
2. V.V. Kashikhin and A.V. Zlobin, "Correction of the Persistent Current Effect in Nb_3Sn Dipole Magnets", IEEE Transactions on Applied Superconductivity, v. 11, No. 1, March 2001, p. 2058.
3. E. Barzi et al., "Study of Nb_3Sn Strands for Fermilab's High Field Dipole Models", IEEE Transactions on Applied Superconductivity, v. 11, No. 1, March 2001, p. 3595.
4. E. Barzi et al., "Instabilities in Transport Current Measurements of Nb_3Sn Strands", IEEE Transactions on Applied Superconductivity, Volume 15, Issue 2, June 2005 Page(s):3364 – 3367
5. C. Boffo, "Magnetization measurements at 4.2K of multifilamentary superconducting strands", FNAL TD-99-0741, Dec.1999.
6. M. D. Sumption et al., "Analysis of Magnetization, AC Loss, and d_{eff} for Various Internal-Sn based Nb_3Sn Multifilamentary Strands with and without Subelement Splitting", Cryogenics, 44 (2004) 711-725.

TABLE 1. Strands Description

Billet ID	8195-97	8079	7054-60	6555	181	187
Technology	RRP	RRP	RRP	RRP	PIT	PIT
No. of filaments	108/127	90/91	54/61	54/61	192	192
Strand diameter, mm	1.0 0.7	0.7	0.7	0.8	1.0	1.0
I_c(12 T), A	~900 ~450	~500	~520	~750	~700	~700
RRR	300 200	300	40	20	>250	>250
Twist pitch, mm	25	-	12	12	20	20
Cu fr., %	49	41	50	~49	52	52

TABLE 2. Cables Description

Cable ID	PITR	PITK	891-A	891-B	891-D	892-A	892-B	892-C	892-D
Strand Technology	PIT	PIT	RRP	RRP	RRP	RRP	RRP	RRP	RRP
No. of strands	28	28	39	39	39	39	39	38	38
Strand diameter, mm	1.0	1.0	0.7	0.7	0.7	0.7	0.7	0.7	0.7
Cable cross-section	Rect.	Keyst.	Keyst.	Keyst.	Keyst.	Rect.	Rect.	Rect.	Rect.
Packing factor, %	88.6	88.6	85	88.5	90	88.5	90	88.5	88

TABLE 3. Effective Filament Diameters and Geometric Filament Sizes

Billet ID	8197	8079	7054-60	6555	181	187
Strand Technology	RRP	RRP	RRP	RRP	PIT	PIT
No. of filaments	107/128	90/91	54/61	54/61	192	192
Strand diameter, mm	1.0	0.7	0.7	0.8	1.0	1.0
D_{eff}, μm	84	72	85	92	50	45
Geometric filament size, μm	63-75	52-65	61-75	-	-	50-57

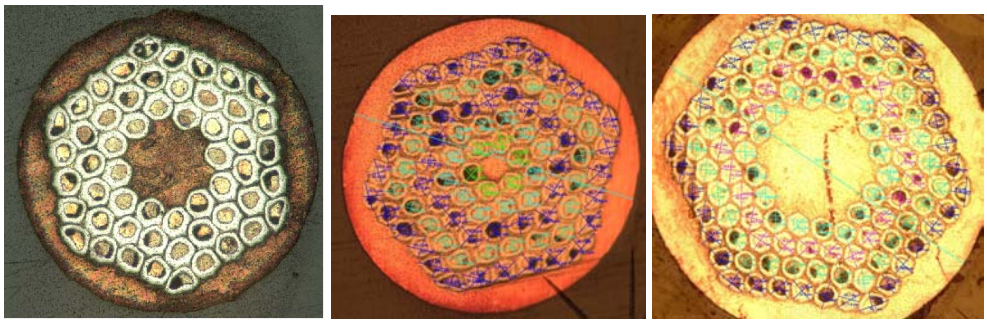

FIGURE 1. 54/61 (left), 90/91 (center) and 108/127 filament (right) RRP designs.

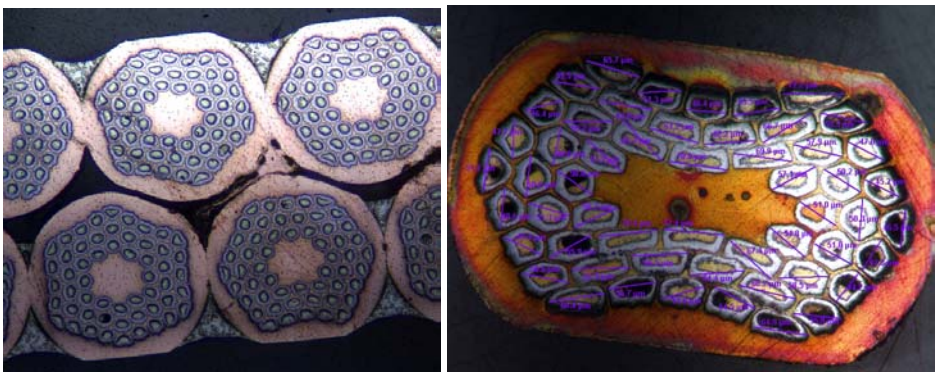

FIGURE 2. RRP unreacted cable (left) and RRP reacted rolled strand (right).

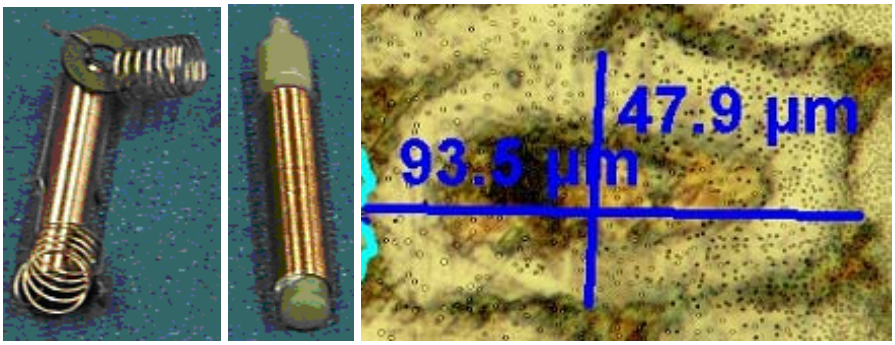

FIGURE 3. Magnetization specimen before reaction (left), and ready for test (center). Short and long diameter measurements on individual filaments (right).

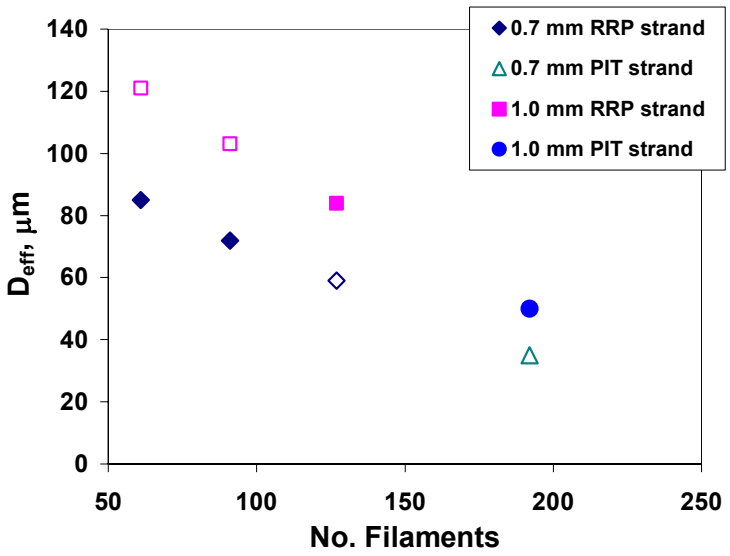

FIGURE 4. D_{eff} as a function of the number of filaments for RRP and PIT strands. Closed markers indicate measured values, open markers indicate values proportionally derived from that measured for the same strand design with different size.

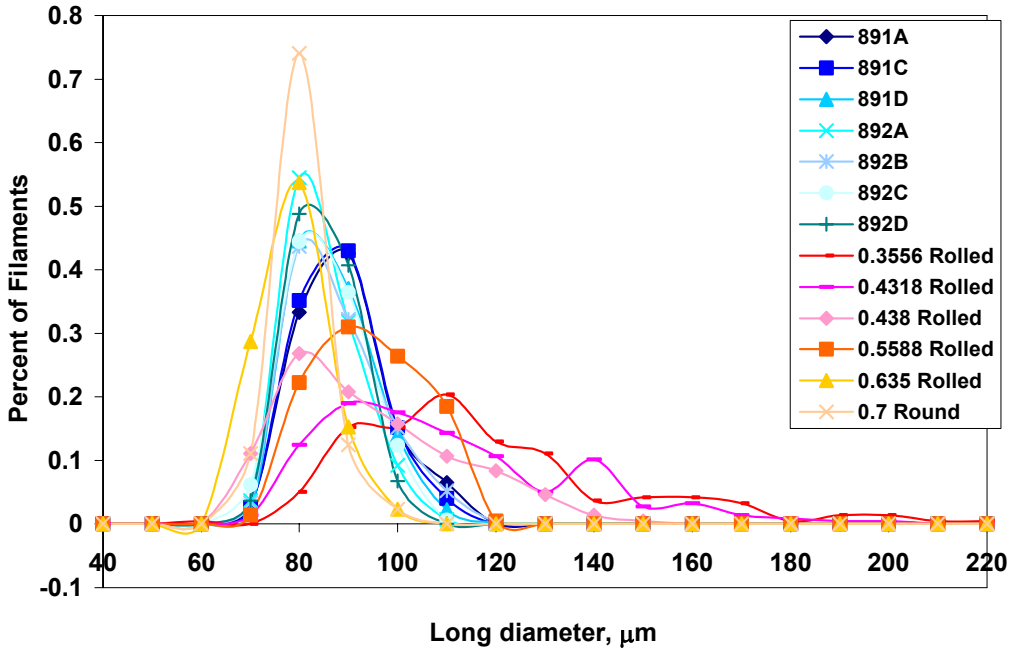

FIGURE 5. Long diameters distributions for 7054-60 RRP round and rolled strands, and from cable cross sections.

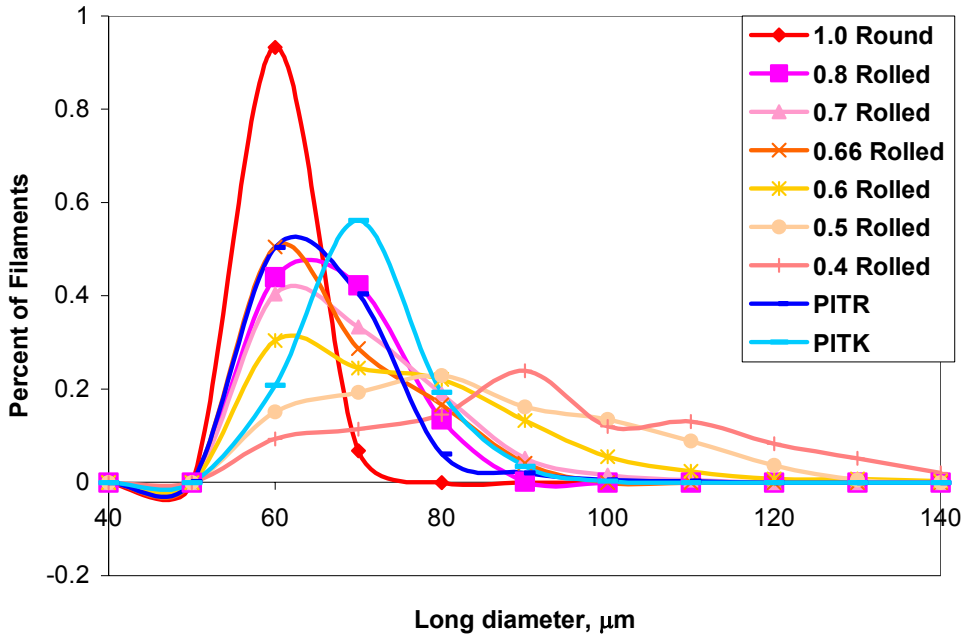

FIGURE 6. Long diameters distributions for PIT round and rolled strands, and from cable cross sections.

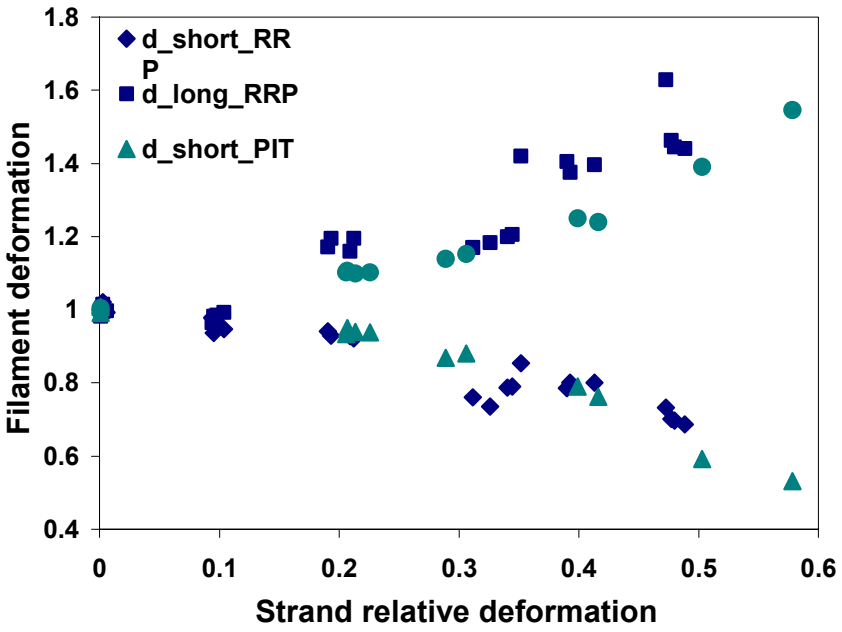

FIGURE 7. Average filament deformation of the short and long diameters as a function of relative strand deformation for both RRP and PIT strands.

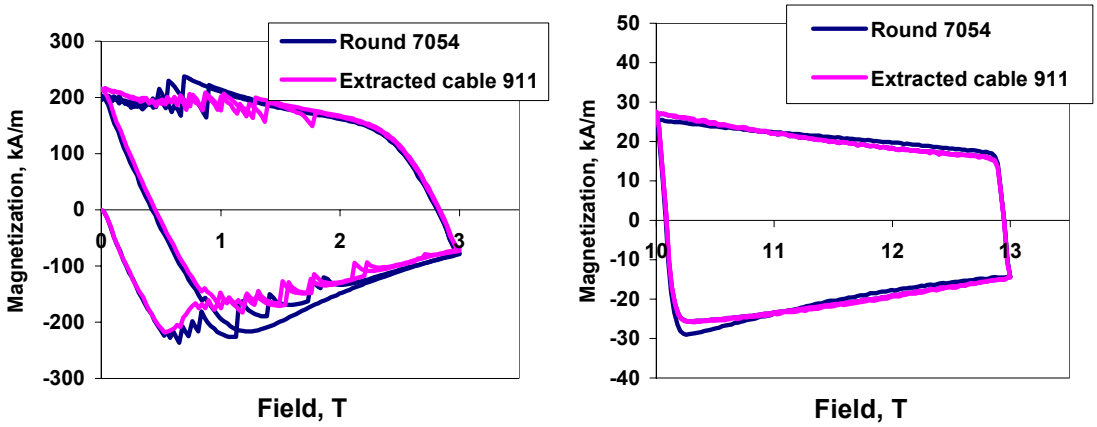

FIGURE 8. Magnetization curves per total volume of an RRP round and extracted strand at low (left) and high field (right).

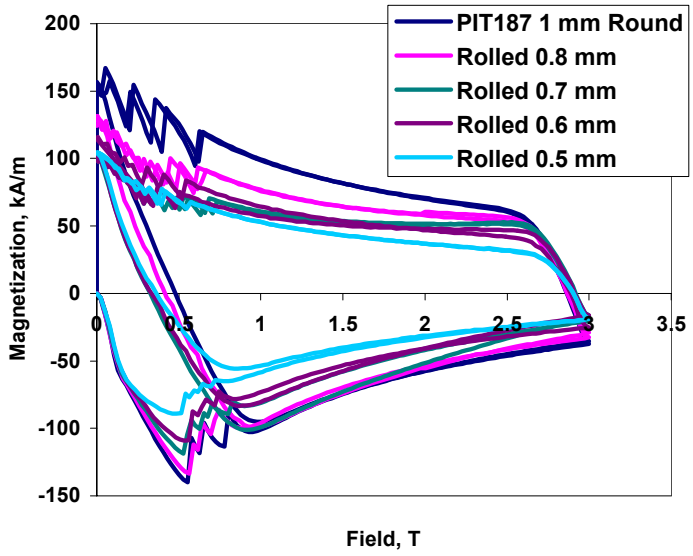

FIGURE 9. Magnetization curves per total volume of PIT187 round and rolled strands at low field.

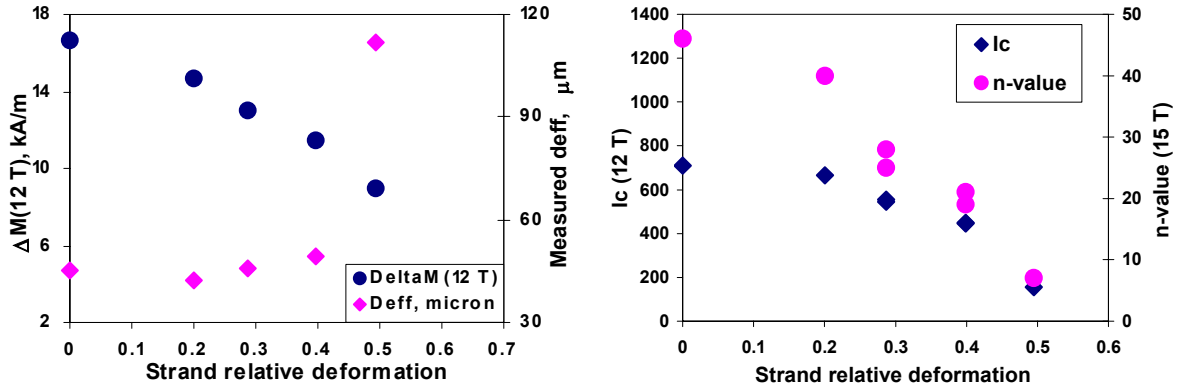

FIGURE 10. ΔM(12 T) and d_{eff} (left), and I_c (12 T) and n-value (15 T) (right) of PIT187 round and rolled strands as a function of relative strand deformation.

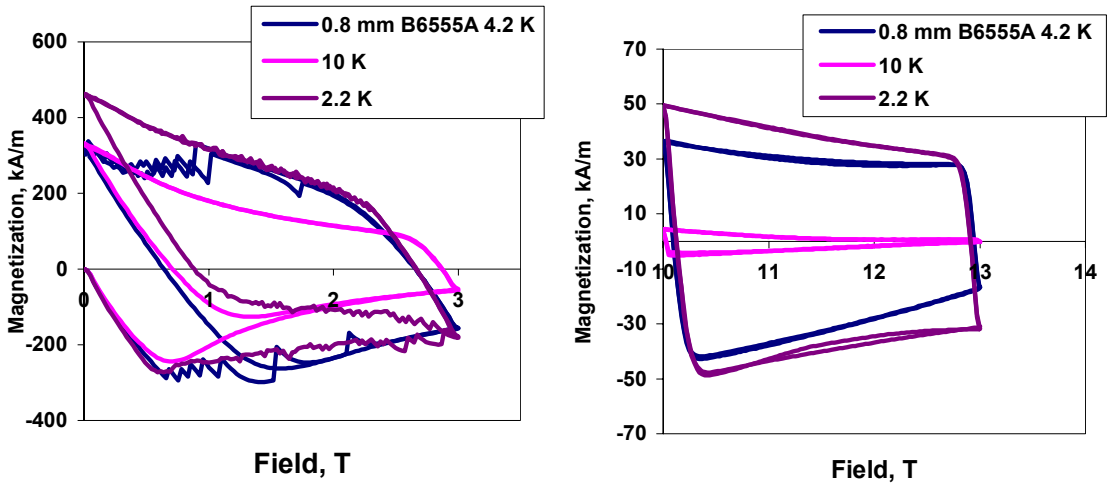

FIGURE 11. Magnetization curves per total volume of an RRP strand at low (left) and high field (right) at 2.2 K, 4.2 K, and 10 K.

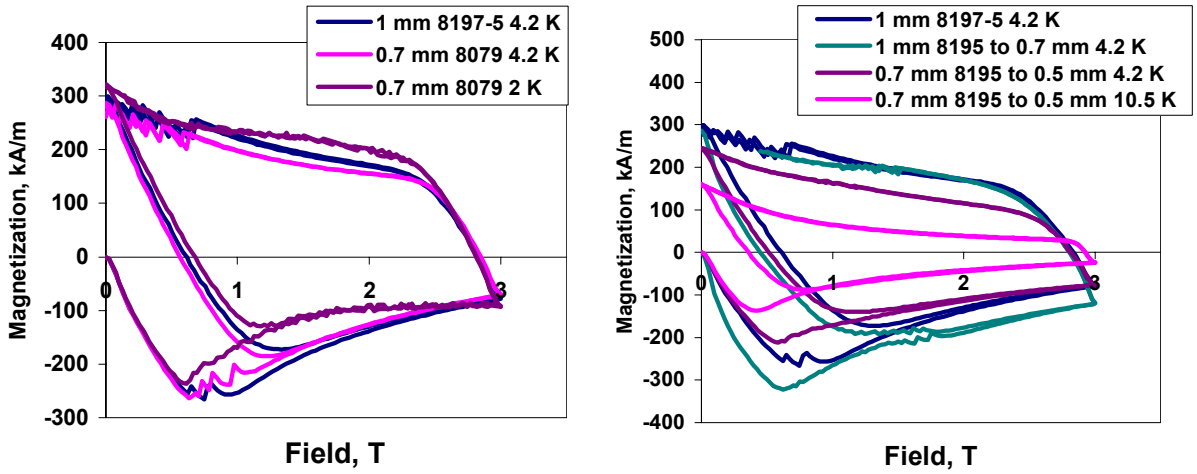

FIGURE 12. Magnetization curves per total volume of round RRP strands at 4.2 K and 2 K (left), and of round and rolled RRP strands at 4.2 K and 10.5 K (right).